Journal of Pharmaceutics & Drug Development
Volume 13 | Issue 1
ISSN: 2348-9782

Research Article Open Access

Pseudotrimezia juncifolia (Klatt) Lovo & A. Gil Effects Against SARS-CoV-2-induced Pulmonary Inflammation

Alan Minho[1#], Pamela Gomes de Almeida[1#], Roberto Fontes Vieira[2], Carolina Batista[3], Isadora Antunes Botelho[4], Daisymara Priscila de Almeida Marques[5], Jordana Grazziela Alves Coelho-dos-Reis[5] and Patricia Dias Fernandes[1*]

[1]Federal University of Rio de Janeiro, Institute of Biomedical Sciences, Laboratory of Pain and Inflammation Pharmacology, Rio de Janeiro, Brazil

[2]Embrapa Genetic Resources and Biotechnology, Biological Station Park, PqEB, Brasília, Brazil

[3]Federal University of Rio de Janeiro, Institute of Biomedical Sciences, Rio de Janeiro, Brazil

[4]Federal University of Rio de Janeiro, Carlos Chagas Filho Institute of Biophysics, Laboratory of Pulmonary Investigation. Rio de Janeiro, Brazil

[5]Federal University of Minas Gerais, Department of Microbiology, Institute of Biomedical Sciences, Laboratory of Basic and Applied Virology, Belo Horizonte, Brazil

[#]Contributed equally to this work

[*]**Corresponding Author:** Patricia Dias Fernandes, Federal University of Rio de Janeiro, Institute of Biomedical Sciences, Laboratory of Pain and Inflammation Pharmacology, Rio de Janeiro, Brazil, E-mail: patricia.dias@icb.ufrj.br

Citation: Alan Minho, Pamela Gomes de Almeida, Roberto Fontes Vieira, Carolina Batista, Isadora Antunes Botelho, et al. (2026) *Pseudotrimezia juncifolia* (Klatt) Lovo & A. Gil Effects Against SARS-CoV-2-induced Pulmonary Inflammation. J Pharma Drug Develop 13(1): 102

Received Date: April 02, 2026 **Accepted Date:** April 22, 2026 **Published Date:** April 25, 2026

Abstract

Pseudotrimezia juncifolia popularly known in Brazil as *ruibarbo* or *beressol*, is an endemic species, particularly found in the Cerrado and Atlantic Forest regions of Brazil. Popular uses for the species have already been reported indicating some different effects such as anti-inflammatory and antinociceptive. We investigated the anti-inflammatory potential of *P. juncifolia* in a murine model of lung inflammation induced by inactivated SARS-CoV-2 (iSARS-CoV-2). Swiss mice received oral treatment with *P. juncifolia* tea at doses of 10, 30, or 100 mg/kg one-hour prior to intranasal instillation of iSARS-CoV-2. After seven days, bronchoalveolar lavage (BAL) fluid and lung tissues were collected to evaluate leukocyte infiltration, protein extravasation, cytokine production, gene expression and histological alterations. Treatment with *P. juncifolia* tea significantly attenuated leukocyte accumulation, decreased protein leakage into BAL fluid, and lower concentrations of inflammatory cytokines. Moreover, treatment downregulated the expression of COX-2, TNF, IL-6, and IFN and reduced NF-κB activation and B1 receptor expression in lung tissue. These findings demonstrate that *Pseudotrimezia juncifolia* exerts significant anti-inflammatory and immunomodulatory effects in experimental SARS-CoV-2–induced lung inflammation, supporting its potential as a therapy targeting excessive inflammatory responses in viral respiratory diseases.

Keywords: *Pseudotrimezia juncifolia*; COVID; SARS-CoV-2; pulmonary inflammation; inflammation

Introduction

SARS-CoV-2 (*Betacoronavirus pandemicum*) is a virus from the coronavirus family that may infect humans, causing a disease called COVID-19. The COVID-19 pandemic, began with an outbreak in Wuhan, China, in November 2019. It spread globally, resulting in millions of cases. Therefore, a comprehensive understanding of the characteristics of COVID-19 remains essential for improving prevention strategies, surveillance efforts, and therapeutic approaches [1]). The virus enters the host cells by binding the SARS-CoV-2 spike protein to the Angiotensin Converting Enzyme-2 (ACE2) receptors in the respiratory epithelium [2].

Viral replication results in virus-mediated tissue damage and host cells triggering an immune response with release of several cytokines. This process can result in a "cytokine storm", occasioning in a local and systemic inflammatory responses [3,4]. It is also observed increase in vascular permeability and activation of the kallikrein-kinin system (KKS) [5,6]. Together, these pathways may evolve to induce respiratory problems, cellular infiltration and even viral pneumonia with similar symptoms of inflammatory levels of pulmonary disease.

Pseudotrimezia juncifolia (Klatt) Lovo & A. Gil (formerly *Trimezia juncifolia*), popularly known in Brazil as *ruibarbo* (rhubarb) or *beressol*, is an herbaceous plant of the *Iridaceae* family, primarily recognized for its ornamental value and traditional medicinal uses. It is endemic to Brazil, particularly found in the Cerrado and Atlantic Forest regions. Popular uses for the species have already been reported, indicating some different effects, such as anti-inflammatory and antinociceptive [7,8].

The aim of this work was to evaluate the effectiveness of *P. juncifolia* tea against SARS-CoV-2-induced pulmonary inflammation. In addition, mechanisms by which *P. juncifolia* tea promoted anti-inflammatory and pro-resolving effects were investigated.

2. Methods

2.1. Animal model

Swiss mice were obtained from the Mice Central Facility of Federal University of Rio de Janeiro. The animals were kept with free access to water and food, in a 12-hour light/dark cycle and controlled temperature (22 ±2 °C). Animals were maintained in the Animal Experimentation Unit of the Institute of Biomedical Sciences/UFRJ. The experimental protocols followed the rules recommended by Law 11.794, of 10/08/2008, by the National Council for the Control of Animal Experimentation (CONCEA) and were approved by the Ethics Committee for the Use of Animals (CEUA) of the Center for Health Sciences/UFRJ (number 93/22).

2.2. Obtaining the inactivated SARS-CoV-2 virus

The SARS-CoV-2 virus, WUHAN strain, was produced in VERO CCL81 cell line at the titer of 1.25×10^6 PFU/ml in a biosafety security level 3 laboratory from Federal University of Minas Gerais. The virus was inactivated by incubation with paraformaldehyde 4% solution for 1h followed by exposure to UV light for another hour. The viral suspension was diluted 5 times in phosphate buffer saline (PBS) to a final concentration of 0.8% paraformaldehyde. The final concentration of paraformaldehyde did not present effect *per se*. Inactivation was confirmed by plaque assay as previously described by our group [9].

2.3. Preparation and Administration of Pseudotrimezia juncifolia

Pseudotrimezia juncifolia (Klatt) Lovo & A. Gil was collected at Botanical Garden, Federal District, Brazil (coordinates 15.880833 and -47.856944 WGS84) at an altitude of 1,113 m. A voucher specimen was deposited in the herbarium of EMBRA-

PA (CEN 120227). Briefly, aerial parts were dried (forced-air oven at 37 °C for 48h) and processed in a knife mill. For preparation of the tea 20 g of powder was infused overnight in boiled distilled water (300 ml). This procedure was repeated three times. The filtrates were pooled, subjected to lyophilization, and stored at -20 °C. On the days of the experiments, dilutions were freshly prepared in distilled water and doses of 10-100 mg/kg (final volume of 0.1 ml per animal) were administered by oral gavage 1h prior of induction of lung inflammation. The control group was composed of mice instilled with saline that received vehicle. The selected doses were based on preliminary studies and prior pharmacological investigations, aiming to cover a range that includes sub-therapeutic to potentially effective doses without inducing toxicity. Additionally, the doses were chosen considering tolerability observed in initial screening assays, ensuring animal safety while allowing the detection of dose-dependent biological effects.

2.4. iSARS-CoV-2-Induced Lung Inflammation

Mice were anesthetized with ketamine/xylazine and received an intranasal instillation of the inactivated virus (10^3 PFU per mice). Animals were maintained in decubitus positions for 10 min and then were returned to the boxes. After 7 days, mice were euthanized with an overdose of ketamine (25 mg/kg)/xylazine (10 mg/kg) solution. A cannula was fixed in the trachea, and 1 ml of sterile PBS was injected and further collected. The bronchoalveolar lavage (BAL) was centrifuged at 1500 rpm, 4 °C, 10 min. Supernatant was collected and stored at −80 °C for several measurements. A group of mice was submitted to perfusion with saline (NaCl 0.9%) and then with paraformaldehyde solution (4%, pH 7.4) to remove all blood. The lungs were collected and frozen for cytokine, histological, and RT-PCR measurements.

2.5. Cytokine assay

Cytokine quantification was performed using specific ELISA kits, the BD OptEIATM Set mouse ELISA, for tumor necrosis factor (TNF), interferon gamma (IFN-γ) and interleukins (IL-6). Concentrations were determined according to the manufacturer's recommendations (B&D Biosciences).

2.6. Quantification of total proteins

The colorimetric method with bicinchoninic acid (BCA) was used [49]. The dosage was performed using the commercial protein quantification kit BCATM Protein Assay (ThermoFisher Scientific, USA).

2.6. RT-qPCR assay

Approximately 100 mg of lung tissue samples were dissociated using an Ultra-turrax homogenizer and total RNA was extracted with Trizol reagent (Sigma, USA), following the manufacturer's instructions. The mRNA concentration was standardized for all samples (50 ng/µl). Analysis of relative gene expression data using real-time quantitative PCR and the $2-\Delta\Delta CT$ method (Livak and Schmittgen, 2001).

2.7. Tissue processing and histology analysis

A laparotomy was promptly conducted, and heparin (1000 IU) was administered into the vena cava. The trachea was clamped at end-expiration (PEEP=2cmH_2O), and the abdominal aorta and vena cava were incised, resulting in a substantial hemorrhage that led to the rapid demise of the animals. Macroscopy was conducted by a pathologist, and gross changes (e.g., size, shape, texture, color) were registered. Lungs were processed using a graded alcohol series, cleaned in xylene, and embedded in paraffin wax. The tissue was cut into 5mm thick slices and stained with hematoxylin and eosin. The slides were scanned in an AxioImager Z2/VSLIDE (Zeiss, Oberkochen, Germany) using 10x and 20x objectives [10]. Photomicrographs at magnifications of x100, x200, and x400 were also captured from four non-overlapping fields of view per section using a light microscope (Olympus BX51, Olympus Latin America-Inc., Brazil).

Diffuse alveolar damage (DAD) was assessed employing a weighted scoring system as previously described [11]. Briefly, scores (0 to 4) were assigned to denote the severity of septal thickening, alveolar collapse, inflammatory infiltration, and hemorrhage, where 0 indicated no effect and 4 represented maximum severity. Scores were computed as the product of the severity and extent of each feature, within a range of 0 to 16. The cumulative DAD score was then calculated as the sum of the scores for each characteristic, ranging from 0 to 64.

Paraffin-embedded lung slides were subjected to antigen retrieval using the citrate buffer protocol at 96 °C for 20 minutes. The slides were removed from the solution after it reached room temperature, and the sections were washed with PBS three times for 5 minutes each time. Non-specific sites were blocked with 5% goat normal serum (Thermo Fischer Co.) and 1% bovine serum albumin (Sigma-Aldrich Co.), diluted in PBS/Triton 0.1% for 2 hours at room temperature, before immunoreaction with the following antibodies: mouse anti-ACE2 monoclonal antibody (1:200, Enzo/Cell Signaling); Monoclonal antibody anti-NF-κB p65 (1:400, Cell Signaling); polyclonal antibody anti-SARS-CoV-2 Spike 1:1,000; Sigma-Aldrich Co.); polyclonal antibody anti-BDKRB1 1:300, Thermo/Bioss); polyclonal antibody anti-B2BKR (1:300, Enzo).

After a period of 8-12h at 4 ºC, the sections were washed with PBS three times, for 5 minutes each wash, and incubated with secondary antibodies in 1% PBS/BSA at room temperature. The secondary antibodies were goat anti-mouse IgG conjugated with Alexa Fluor 488 (1:1,000; Thermo/Invitrogen); goat anti-rabbit IgG conjugated with Alexa Fluor 546 (1:1,000; Thermo/Invitrogen); goat anti-rabbit IgG conjugated with Alexa Fluor 647 (1:1,000; Thermo/Invitrogen). After 2 hours, the sections were washed three times with PBS for 10 minutes each wash, the nuclei were labeled with 4',6'-diamino-2-phenylindole (DAPI; Thermo/Invitrogen) for 10 minutes, and the slides were closed with fluoromount-g mounting medium (Thermo/Invitrogen). The material was kept protected from light at -20°C. The images were captured using a confocal microscope (TCS SPE; Leica), with a 63x objective, and analyzed using Fiji-ImageJ (NIH, Maryland, United States).

2.8. Statistical Analysis

The results are presented as the mean ± standard deviation (n=5-11). Statistical significance between groups was calculated by the student's t-test (non-parametric) followed by Kruskal-Wallis or Tukey tests. P values less than 0.05 (*$p < 0.05$) were considered significant.

3. Results

Instillation of mice with inactivated SARS-CoV-2 (iSARS-CoV-2) resulted in an 80-fold increase in leukocyte infiltration in broncoalveolar space after 7 days. It resulted in a marked and statistically significant increase in total leukocyte numbers when compared with those non-infected animals (control group). While control animals exhibited low baseline leukocyte levels, consistent with physiological homeostasis, infected animals treated with vehicle displayed a pronounced leukocytosis, indicating a strong inflammatory and immune response triggered by viral challenge. The dispersion of individual data points further demonstrates the robustness of this effect across animals within the group.

Treatment of mice with doses of 10, 30, and 100 mg/kg of *P. juncifolia* resulted in a 50% reduction in the number of cells in the broncoalveolar lavage (BAL). Importantly, leukocyte levels in treated groups approached those observed in the saline control group, suggesting partial restoration of inflammatory homeostasis. Although all tested doses were effective, the magnitude of reduction appeared consistent across doses, indicating that the anti-inflammatory effect is maintained within the doses (Figure 1).

It was also observed an increase in vascular permeability resulted in increase in protein levels in BAL. iSARS-CoV-2 instilled mice presented a 2 to 3-fold increase in protein extravasated. Treatment with 10, 30, and 100 mg/kg of *P. juncifolia* significantly

reduced total protein levels compared to untreated infected animals. Notably, protein concentrations in treated groups were substantially lower than in the group of mice receiving inactivated virus and pretreated with vehicle showing a trend toward normalization, indicating protective effects against infection-induced tissue damage (Figure 1).

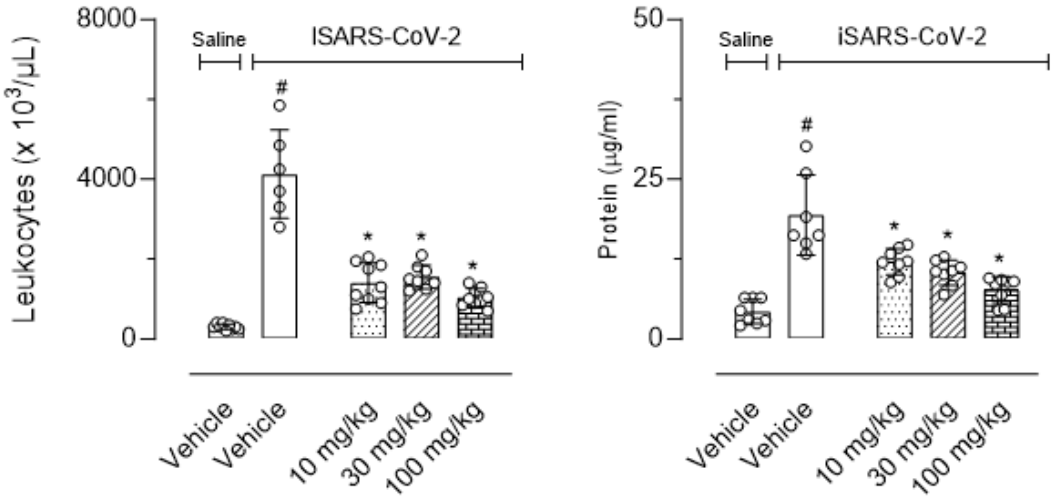

Figure 1: Effect of *P. juncifolia* pretreatment in inflammatory response induced by inactivated SARS-CoV-2 (iSARS-CoV-2). Mice were orally pretreated with tea of *P. juncifolia* (10, 30, or 100 mg/kg) one-hour prior to instillation of iSARS-CoV-2 (10^3 PFU per mice). After 7 days animals were euthanized, broncoalveolar fluids were collected. Leukocytes were counted and protein was measured in supernatant. Results are expressed as mean ± standard deviation (n=6-9). Statistical analyses were performed using GraphPad Prism Software (version 10.1.2) using ordinary One-way ANOVA followed Tukey post-test. # $p < 0.001$ when comparing iSARS-CoV-2 instilled mice treated with vehicle with saline-instilled mice treated with vehicle. * $p < 0.001$ when comparing iSARS-CoV-2 instilled mice that were treated with *P. juncifolia* with iSARS-CoV-2 instilled mice treated with vehicle.

Figure 2 shows the effects of treatment with *P. juncifolia* in production of cytokines (TNF, IL-6, and IFN) in iSARS-CoV-2 infected mice. Animals that were instilled with saline and received pretreatment with vehicle exhibited low cytokine levels, consistent with physiological homeostasis. In contrast, instillation with iSARS-CoV-2 significantly increased the concentrations of all three cytokines, demonstrating an inflammatory process induced by viral challenge.

TNF levels were markedly elevated in animals receiving iSARS-CoV-2 instillation and pretreated with vehicle, reaching values higher than those observed in control groups. Treatment with *P. juncifolia* (at 10, 30, and 100 mg/kg) significantly reduced TNF concentrations. A similar pattern was observed for IL-6 production. Instillation of iSARS-CoV-2 resulted in an increase in IL-6 levels, confirming activation of inflammatory signaling pathways commonly associated with acute viral infection. Administration of *P. juncifolia,* at all tested doses, significantly decreased IL-6 concentrations relative to untreated infected animals, suggesting effective modulation of cytokine production. The reduction appeared consistent across doses, with a tendency toward partial normalization. Regarding IFN levels, iSARS-CoV-2 infection induced a significant increase compared to control animals. Treatment with 10, 30, and 100 mg/kg of *P. juncifolia* significantly reduced IFN concentrations. Despite this reduction, IFN levels in treated animals remained above baseline values, indicating modulation rather than complete suppression of the antiviral response.

Next, we decided to analyze whether there would be changes in expression of some genes involved in the inflammatory process. The figure 3 shows the relative gene expression levels of COX-2, IFN, IL-6, and TNF, expressed as $-\Delta\Delta CT$ values.

Basal genes expression was observed in all groups reflecting physiological transcriptional homeostasis. In contrast, after instillation of iSARS-CoV-2 a significantly upregulation in the expression of all genes were observed, suggesting activation of pro-inflammatory and innate immune signaling pathways at the transcriptional level. Treatment with *P. juncifolia* (at 10, 30, or 100 mg/kg) significantly reduced COX-2 expression when compared to untreated infected animals. It is interesting to note that the highest dose reduced COX-2 to basal levels (Figure 3).

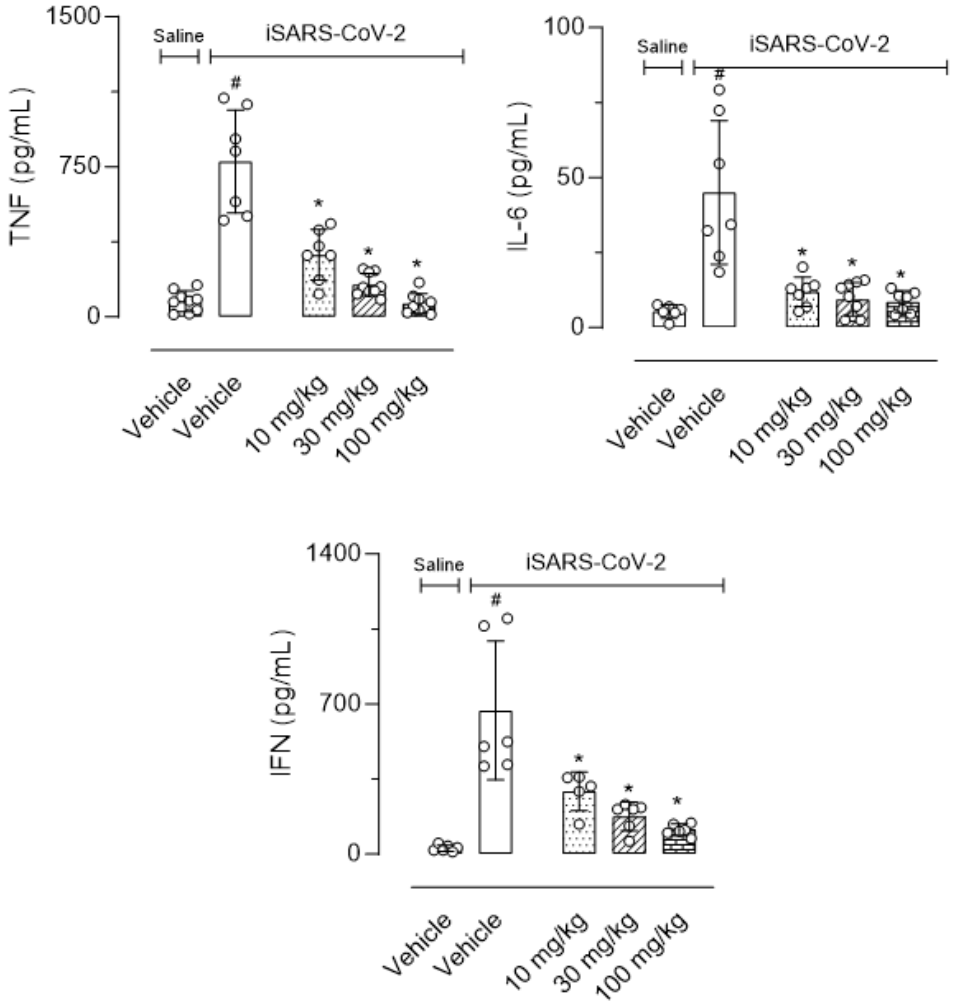

Figure 2: *Pseudotrimezia juncifolia* pretreatment reduces levels of cytokine after instillation of inactivated SARS-CoV-2 (iSARS-CoV-2). Mice were oral pretreated with tea of *P. juncifolia* (10, 30, or 100 mg/kg) one-hour prior to instillation with iSARS-CoV-2 (10^3 PFU per mice). After 7 days animals were euthanized, broncoalveolar fluids were collected. Tumor necrosis factor (TNF), interleukin-6 (IL-6), and interferon (IFN) were measured in the supernatant of the broncoalveolar fluid collected. Results are expressed as mean ± standard deviation (n=6-9). Statistical analyses were performed using GraphPad Prism Software (version 10.1.2) using ordinary One-way ANOVA followed Tukey post-test. # $p < 0.001$ when comparing iSARS-CoV-2 instilled mice treated with vehicle with saline-instilled mice treated with vehicle. * $p < 0.001$ when comparing iSARS-CoV-2 instilled mice that were treated with *P. juncifolia* with iSARS-CoV-2 instilled mice treated with vehicle.

Similarly, IFN gene expression was elevated after virus instillation and the administration of the *P. juncifolia* significantly decreased IFN mRNA levels suggesting modulation of the antiviral transcriptional response. Although expression remained above basal levels, the reduction suggests controlled regulation rather than complete inhibition of interferon signaling.

IL-6 mRNA levels were also significantly increased in the iSARS-CoV-2 instilled group. All three doses of *P. juncifolia* did significantly downregulate IL-6 expression suggesting suppression of IL-6-driven inflammatory signaling (Figure 3).

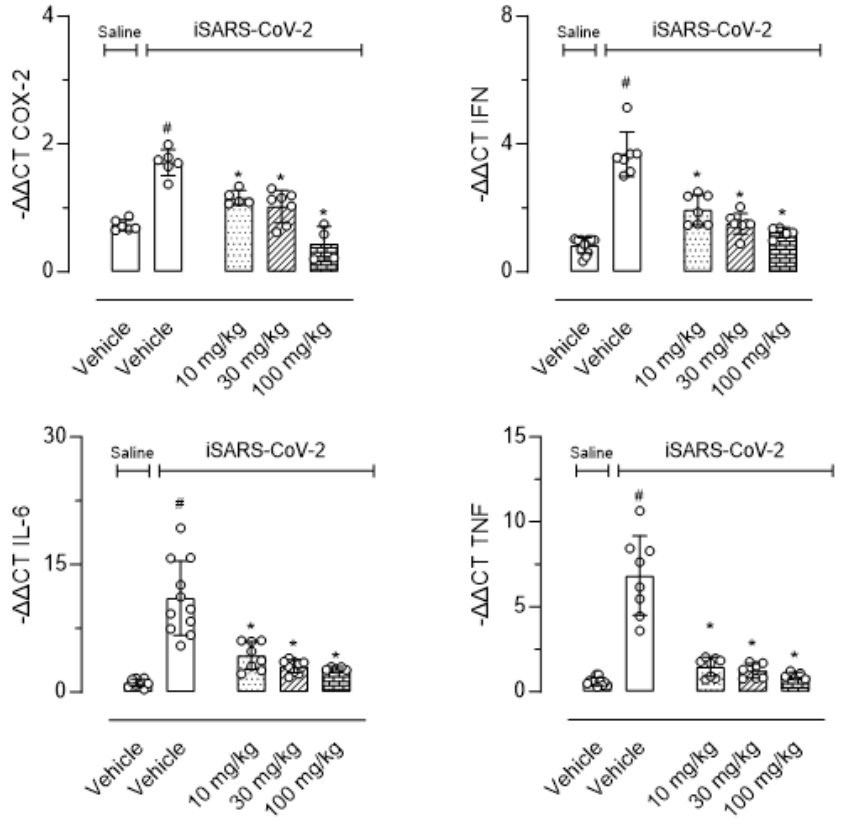

Figure 3: *Pseudotrimezia juncifolia* pretreatment reduces mRNA levels of COX-2, IFN, IL-6, and TNF after instillation of inactivated SARS-CoV-2 (iSARS-CoV-2). Mice were pretreated with tea of *P. juncifolia* (10, 30, 100 mg/kg) one-hour prior to instillation with iSARS-CoV-2 (10^3 PFU per mice). After 7 days animals were euthanized, and lungs collected. mRNA levels of cyclooxygenase-2 (COX-2), tumor necrosis factor (TNF), interleukin-6 (IL-6) and interferon (IFN) were measured in lungs of mice. Results are expressed as mean ± standard deviation (n=6-9). Statistical analyses were performed using GraphPad Prism Software (version 10.1.2) using ordinary One-way ANOVA followed Tukey post-test. # $p < 0.001$ when comparing iSARS-CoV--2 instilled mice treated with vehicle with saline-instilled mice treated with vehicle. * $p < 0.001$ when comparing iSARS-CoV-2 instilled mice that were treated with *P. juncifolia* with iSARS-CoV-2 instilled mice treated with vehicle.

Table 1: Diffuse Alveolar Damage Score (DAD)

	Intranasal installation of				
	Saline	iSARS-CoV-2			
Groups	Vehicle (a)	Vehicle (b)	10 mg/Kg	30 mg/kg	100 mg/kg
Alveolar Edema	1.06 (1.0-1.3)	2.18 (1.3-3.5)#	1.42 (1.2-1.6)	1.22 (1.1-1.4)	1.08 (1.0-1.2)*
Alveolar Thickening	4.60 (2.6 – 5.9)	6.70 (6.2 – 7.2)#	5.35 (4.4–6.6)	5.55 (4.4–6.6)	4.60 (4.0– 5.2)*
Inflamatory infiltration	3.02 (2.5 – 3.6)	5.85 (4.8 – 6.9)#	4.50 (3.6–5.5)	5.07 (4.5–5.6)	3.37 (2.6–4.00*
Hemorrhage	1.00 (1.0-1.0)	1.06 (1.0 – 1.3)	1.12 (1.0–1.4)	1.05 (1.0–1.1)	1.06 (1.0–1.1)
Total DAD	10.26 (8.2 – 11.4)	15.88 (14.6 – 17.6)#	12.80 (10.8–14.1)	12.38 (10.4–14.2)	10.28 (9.4–12.1)*

We next decided to evaluate the effect of *P. juncifolia* treatment on alveolar damage. The diffuse alveolar damage score (DAD), an indication of severity of pulmonary edema, septal thickening, inflammatory infiltrate, and hemorrhage was calculated. It can be observed that instillation of inactivated virus did not cause hemorrhage in mice. However, it significantly induced an increase in inflammatory infiltrate, alveolar edema, and alveolar thickening. Pretreatment of animals with doses of 10 or 30 mg/kg did not affect the parameters. But it is interesting to note that 100 mg/kg dose reduced all three parameters to levels similar to the control group (Figure 4 and table 1).

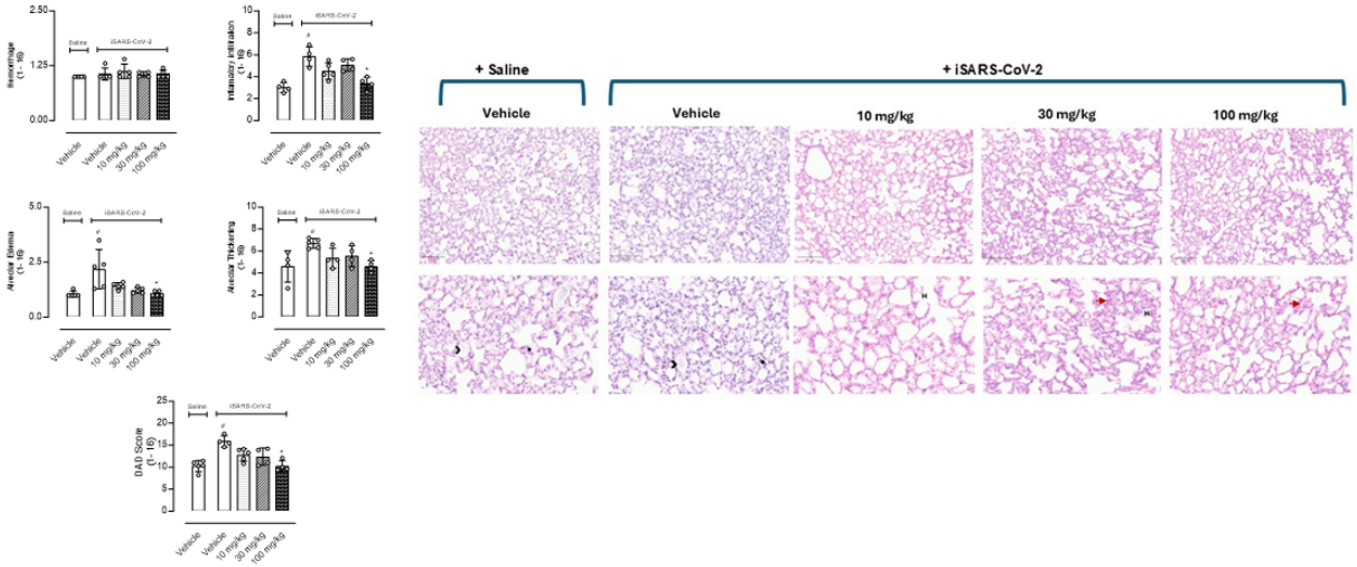

Figure 4: Effect of *P. juncifolia* treatment in hemorrhage, inflammatory infiltrate, alveolar edema, alveolar thickening, and Diffuse Alveolar Damage Score (DAD) after inflammatory response induced by iSARS-CoV-2. Mice were instilled with inactivated SARS-CoV-2 (iSARS-CoV-2, 10^3 PFU per mice). One-hour prior-installation mice were orally-treated with *P. juncifolia* (10, 30, 100 mg/kg). After 7 days animals were euthanized, and lungs collected and processed. Results are expressed as mean ± standard deviation (n=4-5). Statistical analyses were performed using GraphPad Prism Software (version 10.1.2) using ordinary One-way ANOVA followed Tukey post-test. # $p < 0.05$ when comparing iSARS-CoV-2 instilled mice treated with vehicle with saline-instilled mice treated with vehicle. * $p < 0.05$ when comparing iSARS-CoV-2 instilled mice that were treated with *P. juncifolia* with iSARS-CoV-2 instilled mice treated with vehicle. Images are representative photomicrographs of lung stained with hematoxylin and eosin from the groups. Upper panels images were taken at 40x magnification and bars represent 100μm. Lower panels images were taken at 40x magnification and bars represent 50μm. Red arrow: inflammatory infiltration; H: hemorrhage; Black arrow: Edema; Asterisk: Septal thickening.

We then decided to evaluate alterations induced by iSARS-CoV-2 and the effects of *P. juncifolia* pretreatment in expression of some receptors. We did not observe the presence of the virus in the lung parenchyma in all experimental conditions (Figure 5), However, the data presented indicate that, even without the presence of viral particles, there is an inflammatory environment.

The qualitative analysis of Angiotensin converting enzyme-2 (ACE2) staining does not show a difference between the experimental conditions, but the analysis of the fluorescence intensity of lung sections indicates that treatment with *P. juncifolia* decreases the presence of the cellular form of ACE2, at levels lower than that found in the lungs of control animals and in the group of animals that were instilled with the inactivated virus. All groups (instilled with iSARS-CoV-2 and treated with *P. juncifolia*) show an increase in Bradykinin receptor-2 (B2R) fluorescence intensity when compared to the group instilled with saline and pretreated with vehicle (Figure 5).

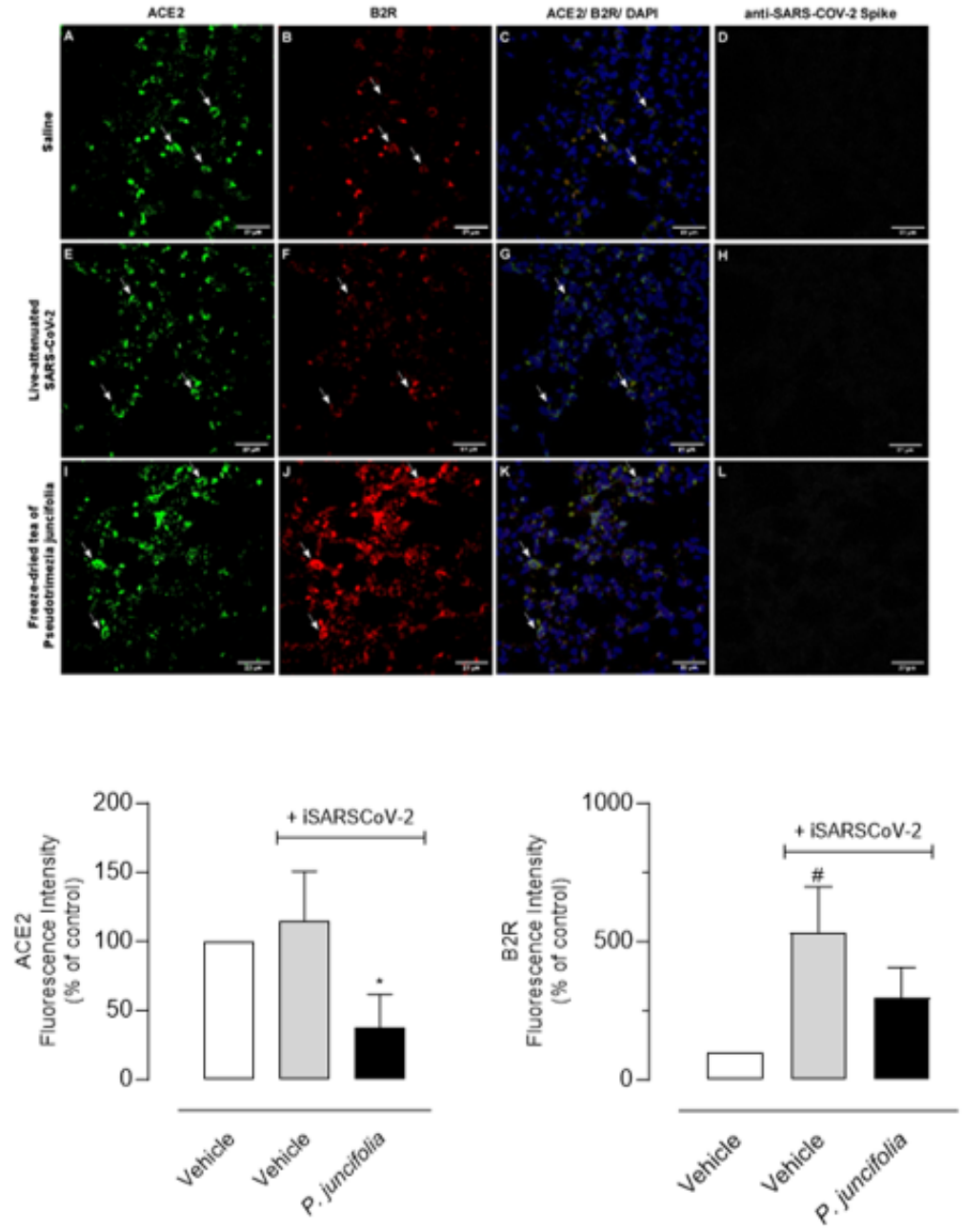

Figure 5: Labeling of spike SARS-CoV-2 protein, Angiotensin converting enzyme-2 (ACE2), and bradykinin receptor-2 (B2R) in the lung parenchyma. Mice were pretreated with *P. juncifolia* (100 mg/kg) one-hour prior to instillation with inactivated SARS-CoV-2 virus (iSARS-CoV-2) (10^3 PFU per mice). After 7 days animals were euthanized, and lungs collected. Images are representative of four collected images. Tissues were incubated with antibodies against ACE2, BKR2, spike protein or DAPI. Fluorescence was quantified as described in methods section. The arrows indicate double labeling, showing that the labels are on the same cell. Results are expressed as mean ± standard deviation. Statistical analyses were performed using GraphPad Prism Software (version 10.1.2) using ordinary One-way ANOVA followed Tukey post-test. # $p < 0.001$ when comparing iSARS-CoV-2 instilled mice treated with vehicle with saline-instilled mice treated with vehicle. * $p < 0.001$ when comparing iSARS-CoV-2 instilled mice that were treated with *P. juncifolia* with iSARS-CoV-2 instilled mice treated with vehicle.

Like B2R, there was an increase in the fluorescence intensity of B1R when animals were instilled with iSARS-CoV-2. Treatment with *P. juncifolia* reduced the expression of the receptor to levels similar to the vehicle-treated group (Figure 6). Since the transcription factor NF-κB is associated with B1R transcription, labeling analysis of this protein was performed. Semi-quantitative

analysis of the fluorescence intensity indicates an increase in the transcription factor in the lung parenchyma of animals instilled with the iSARS-CoV-2. We also observed a reduction in the levels of NF-κB in those mice treated with *P juncifolia* (Figure 6). The increase in B1R and the absence of an increase in ACE2 in the lungs of animals that received the virus indicate DBK activity, since there is no increase in ACE2 to hydrolyze the peptide.

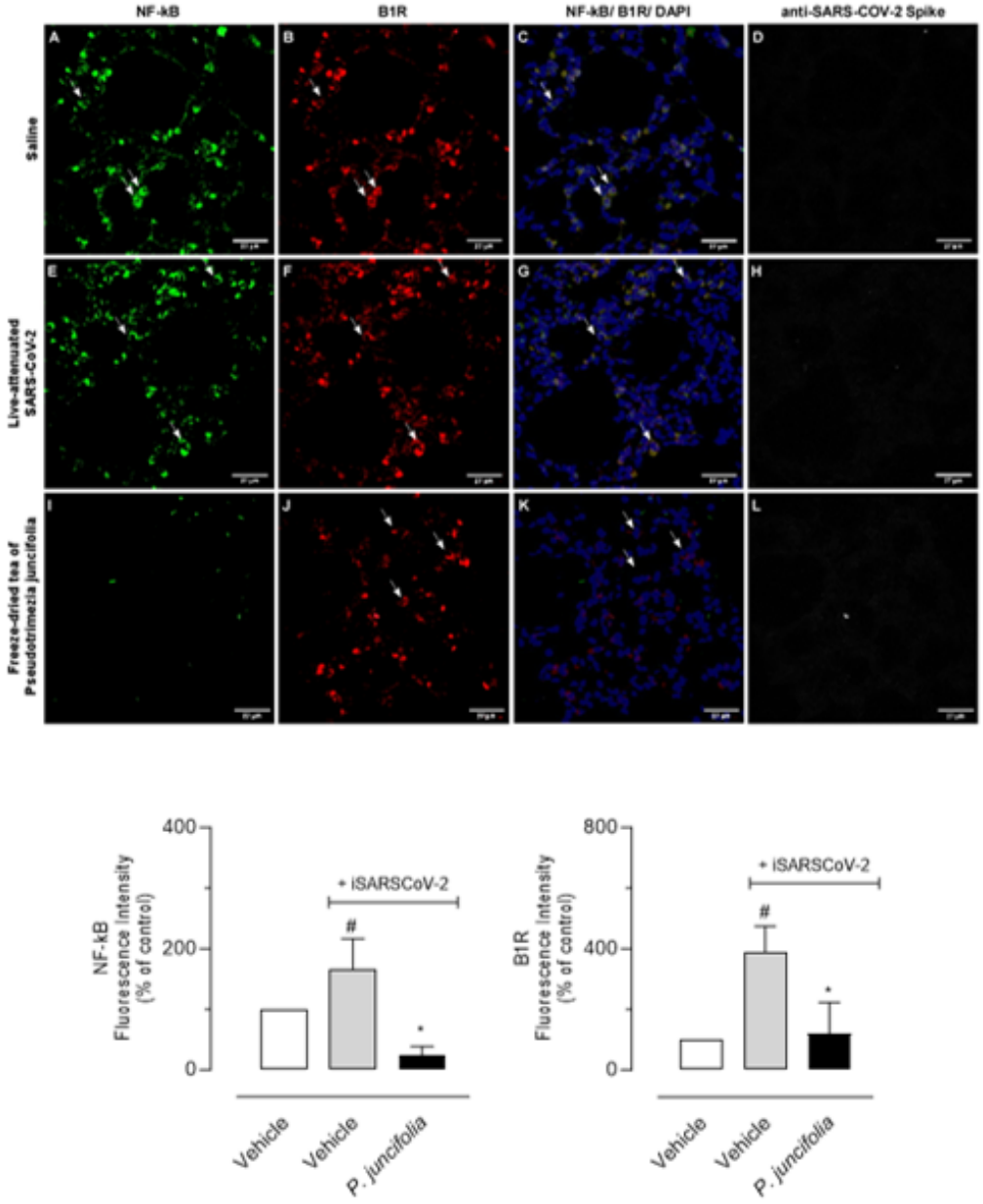

Figure 6: Labeling of NF-kB and bradykinin receptor-1 (B1R) in the lung parenchyma. Mice were pretreated with *P. juncifolia* (100 mg/kg) one hour prior to instillation with inactivated SARS-CoV-2 virus (iSARS-CoV-2) (10^3 PFU per mice). After 7 days animals were euthanized, and lungs collected. Images are representative of four collected images. Tissues were incubated with antibodies against NFkB, B1R, and DAPI. Fluorescence was quantified as described in methods section. The arrows indicate double labeling, showing that the labels are on the same cell. Results are expressed as mean ± standard deviation. Statistical analyses were performed using GraphPad Prism Software (version 10.1.2) using ordinary One-way ANOVA followed Tukey post-test. # $p < 0.001$ when comparing iSARS-CoV-2-instilled mice treated with vehicle and with saline-instilled mice treated with vehicle. * $p < 0.001$ when comparing iSARS-CoV-2 instilled mice that were treated with *P. juncifolia* with iSARS-CoV-2 instilled mice treated with vehicle.

Discussion

The present study shows that administration of *Pseudotrimezia juncifolia* tea reduces pulmonary inflammation triggered by intranasal instillation of inactivated SARS-CoV-2 (iSARS-CoV-2) in mice. Although the virus used in this experimental model is unable to replicate, the findings demonstrate that viral structural elements alone can initiate an inflammatory response in lung tissue. The use of the inactivated SARS-CoV-2 model was chosen as a safe and well-established approach to investigate inflammatory and nociceptive responses associated with viral components, without the need for high-level biosafety containment. This model preserves key structural proteins of the virus, allowing the activation of relevant immune pathways, including those mediated by pattern recognition receptors, which are known to contribute to the pathophysiology of COVID-19-related inflammation and pain. Therefore, it represents a suitable and reproducible experimental platform for evaluating anti-inflammatory and antinociceptive compounds. This observation aligns with evidence indicating that pathogen-associated molecular patterns (PAMPs) derived from viruses including structural proteins and viral RNA fragments can activate innate immune sensors such as Toll-like receptors and cytosolic RNA-recognition pathways. Activation of these receptors subsequently triggers inflammatory signaling cascades even in the absence of viral replication [11,12].

In the current model, exposure to iSARS-CoV-2 resulted in an important increase in leukocyte accumulation within the bronchoalveolar compartment. This response reflects the activation of pulmonary innate immune mechanisms by viral components. Clinical studies of COVID-19 have similarly reported marked infiltration of inflammatory cells in lung tissue, which contributes to alveolar injury, disruption of epithelial barrier integrity, and impaired respiratory function [13,14].

Importantly, treatment with *P. juncifolia* significantly decreased leukocyte recruitment into the bronchoalveolar space. This finding suggests that the tea exerts anti-inflammatory activity reduces immune cell migration into the lungs. This effect is particularly relevant because uncontrolled leukocyte infiltration contributes to pulmonary damage through the release of proteolytic enzymes, reactive oxygen species, and pro-inflammatory mediators. Therefore, the ability to restrain inflammatory cell accumulation may represent an important protective mechanism during virus-induced lung inflammation.

The anti-inflammatory activity observed in the present work is consistent with previous studies conducted by our group investigating the pharmacological properties of *P. juncifolia*. In earlier experiments, extracts obtained from this plant displayed significant anti-inflammatory effects in classical preclinical models of inflammation [8]. The similarity between those observations and the results reported here suggests that the biological activity of *P. juncifolia* is not limited to a specific inflammatory stimulus or tissue. Rather, the plant appears to possess broader immunomodulatory properties regulating inflammatory processes across different biological systems.

In addition to promoting leukocyte infiltration, exposure to iSARS-CoV-2 also impaired pulmonary vascular integrity, as demonstrated by the elevation of protein levels in bronchoalveolar lavage (BAL) fluid. The presence of plasma proteins is recognized as a marker of inflammatory lung injury and indicates increased permeability of the alveolar-capillary barrier. This phenomenon is commonly observed in severe viral pneumonia and represents a key pathological feature of acute respiratory distress syndrome (ARDS), one of the most serious complications associated with COVID-19 [15]. In the present study, animals exposed to iSARS-CoV-2 showed a two- to three-fold increase in BAL protein concentrations, indicating significant disruption of pulmonary barrier function.

Treatment with *P. juncifolia* markedly reduced protein leakage into BAL fluid, suggesting that the plant may protect against inflammation-associated vascular dysfunction. Interestingly, these observations are consistent with previous findings from our group, in which *P. juncifolia* extracts were shown to significantly decrease protein extravasation in experimental models of inflammation. The reproducibility of this effect supports the hypothesis that compounds present in *P. juncifolia* may contribute

to maintaining vascular integrity during inflammatory responses. In the context of pulmonary inflammation, preservation of alveolar barrier function is particularly important, as it may reduce edema formation and mitigate respiratory impairment.

Another important component of the inflammatory response investigated in this study was cytokine production. Exposure to iSARS-CoV-2 led to elevated levels of TNF, IL-6, and IFN. These mediators play critical roles in antiviral defense; however, their excessive production may promote tissue injury. In severe cases of COVID-19, high systemic concentrations of inflammatory cytokines have been associated with the development of the so-called cytokine storm, characterized by uncontrolled systemic inflammation and multi-organ dysfunction [13,16].

Administration of *P. juncifolia* significantly reduced TNF and IL-6 concentrations in BAL fluid. These findings agree with our previous results showing that *P. juncifolia* markedly suppresses TNF production in experimental inflammation models [8]. The consistent inhibition of inflammatory cytokines across different experimental settings suggests that the plant may act on upstream signaling pathways responsible for regulating cytokine synthesis.

Interestingly, although IFN levels were also reduced after treatment with *P. juncifolia*, they remained higher than those observed in control animals. This observation is particularly noteworthy since interferons play essential roles in antiviral immunity by inducing interferon-stimulated genes that limit viral replication and enhance host defense mechanisms. Complete inhibition of interferon signaling could compromise antiviral responses. Therefore, the partial reduction observed in this study may indicate an immunomodulatory effect rather than broad immunosuppression. Such balanced regulation of inflammatory pathways has been proposed as an advantageous therapeutic strategy in viral infections where excessive inflammation contributes significantly to disease severity [17].

Gene expression analysis of lung tissue further supported the anti-inflammatory activity of *P. juncifolia*. Instillation of iSARS--CoV-2 significantly increased the transcription of inflammatory mediators, including COX-2, TNF, IL-6, and IFN, indicating activation of innate immune signaling pathways.

Histological and immunofluorescence analyses provided additional insight into the mechanisms involved in the *P. Juncifolia* effects. Even in the absence of detectable viral replication within lung tissue, an inflammatory environment was observed. This finding reinforces the concept that viral structural elements alone can activate inflammatory signaling pathways independently of viral replication. A particularly relevant observation was the activation of the kallikrein–kinin system (KKS). Increased fluorescence signals for bradykinin receptors (B1R) and B2R were detected in animals exposed to iSARS-CoV-2, indicating activation of this pathway during pulmonary inflammation. KKS is known to regulate vascular permeability, vasodilation, and inflammatory cell recruitment. Dysregulation of this system has been proposed as an important mechanism contributing to pulmonary inflammation and vascular leakage during COVID-19 [18].

The expression of B1R observed in the lungs of animals exposed to iSARS-CoV-2 is particularly relevant because this receptor is typically upregulated under inflammatory conditions. Activation of B1R has been associated with enhanced cytokine production, increased leukocyte migration, and greater vascular permeability [19].

Signaling mediated by bradykinin receptors is closely connected to NF-κB-dependent inflammatory pathways. Binding of bradykinin to B2R can promote phosphorylation and degradation of IκBα, allowing nuclear translocation of NF-κB and activation of inflammatory gene transcription [20]. This signaling cascade can also activate phospholipase A_2 and cyclooxygenase pathways, resulting in the production of prostaglandins and other inflammatory mediators. Through these mechanisms, activation of the KKS may amplify inflammatory responses by establishing a positive feedback loop between bradykinin signaling and NF-κB-mediated cytokine production. In turn, cytokines such as TNF and IL-6 can further stimulate expression of inducible receptors such as B1R, thereby perpetuating inflammatory signaling [21,22]. The findings obtained in the present study are

consistent with the involvement of this interconnected signaling network. Exposure to iSARS-CoV-2 resulted in increased cytokine production, enhanced expression of B1 and B2 receptors, and activation of NF-κB in lung tissue.

Polyphenols are the predominant secondary metabolites among the 44 compounds identified in the lyophilized tea of *P. juncifolia*, being mostly composed of flavonoids, proanthocyanidins and chlorogenic acids and their derivatives, such as epigallocatechin, luteolin, catechin, taxifolin, myricetin-3-O-rutinoside, myricetin-3-O-glucoside, rutin, isoorientin, procyanidin B2, procyanidin C1, clitorin, loliolide, among others [8]. Among the compounds identified, some are common in many plants such as epigallocatechin which has been identified in blackberry, sweet cherry and *Solanum lycopersicum* (tomato) [23], *Acacia mearnsii* [24], *Rhodiola semenovii* [25], *Rhodiola semenovii* (peanut) [26], and green tea [27]. For this phytochemical compound present in some extracts and teas, it has described some pharmacological properties such as anti-inflammatory and antioxidant activity, in the treatment of obesity and cardiovascular diseases and the effect on the stabilization of mast cells. Another compound, luteolin observed in the phytochemistry of *Paeonia rockii* [28]; is also present in *Paeonia lactiflora* Pal [29], as well as in *Portulaca oleracea* L. and *Porophyllum ruderale* (Jacq.) Cass [30]. Many plants that have shown some pharmacological effect have luteolin in their phytochemical characterization, such as antioxidant, anti-inflammatory, antibacterial and antimigratory activity, protection and repair of oxidative damage to DNA, chemoprotective, antiviral, anticancer, anti-neurodegenerative, among others [31,32].

To the best of our knowledge this work was the first report to demonstrate that *Pseudotrimezia juncifolia* tea significantly reduced pulmonary inflammation induced by inactivated SARS-CoV-2. Treatment reduces leukocyte infiltration, preserves vascular barrier integrity, suppresses cytokine production, downregulates inflammatory gene expression, and modulates signaling pathways involving NF-κB and the KKS. Together these findings support the potential of *P. juncifolia* as a promising species for treating and controlling virus-induced inflammatory diseases.

Acknowledgement

To Pulmonary Research Laboratory, Instituto de Biofísica Carlos Chagas Filho for the use of AxioImager Z2/VSLIDE cell scanner equipment.

Funding

This work was supported by to the Brazilian Agencies - Conselho Nacional de Desenvolvimento Científico e Tecnológico (CNPq, #406739-2018-8, #303804-2020-3, #306900/2023-8, Brazil) to PDF (fellowships and grant support), Fundação Carlos Chagas Filho de Apoio à Pesquisa (FAPERJ, Brazil) to PDF (grant support). JGCdR and PDF received PG Fellowships from CNPq.

Competing Interests

The authors declare no competing interests.

Data Availability

The data underlying this article are available in the article

Author contributions statement

PDF - conceptualization, formal analysis, data curation, funding acquisition, project administration, resources, supervision,

writing – original draft and review and editing.

JGACR – methodology, review and editing.

AM, PGA, RFV, C.B, I.A.B. D.P.A.M.- Investigation, Methodology

References

1. Wu Z, McGoogan JM (2020) Characteristics of and important lessons from the coronavirus disease 2019 (COVID-19) outbreak in China. JAMA, 323: 1239–42.

2. Xu H, et al. (2020) High expression of ACE2 receptor of 2019-nCoV on the epithelial cells of oral mucosa. Int J Oral Sci, 12: 8.

3. Azkur AK, et al. (2020) Immune response to SARS-CoV-2 and mechanisms of immunopathological changes in COVID-19. Allergy, 75: 1564-81.

4. Wang J, et al. (2020) Cytokine storm and leukocyte changes in mild versus severe SARS-CoV-2 infection: Review of 3939 COVID-19 patients in China and emerging pathogenesis and therapy concepts. J Leukoc Biol, 108: 17-41.

5. Ackermann M, et al. (2020) Pulmonary Vascular Endothelialitis, Thrombosis, and Angiogenesis in Covid-19. N Engl J Med, 383: 120-8.

6. Teuwen LA, et al. (2021) COVID-19: the vasculature unleashed. Nat Rev Immunol, 20: 389-91.

7. Fagg CW, et al. (2015) Useful Brazilian plants listed in the manuscripts and publications of the Scottish medic and naturalist George Gardner (1812-1849). J Ethnopharmacol, 23: 18-29.

8. Minho AS, et al. (2024) Anti-Inflammatory, Antinociceptive, and LC-MS Metabolic Profile from Pseudotrimezia juncifolia (Klatt) Lovo &A. Gil. Pharmaceuticals, 17: 1101.

9. Marques DPA, et al. (2024) New anti-SARS-CoV-2 aminoadamantane compounds as antiviral candidates for the treatment of COVID-19. Virus Res, 340: 199291.

10. Rodrigues SC, et al. (2021) Toxicological profile of umbilical cord blood-derived small extracellular vesicles. Membranes, 11: 9.

11. Hsia CCW (2010) An official research policy statement of the American Thoracic Society/European Respiratory Society: Standards for quantitative assessment of lung structure. Am J Resp Crit Care Med, 181: 394–418.

12. Merad M, Martin JC (2020) Pathological inflammation in patients with COVID-19: A key role for monocytes and macrophages. Nature Rev Immunol, 20: 355–62.

13. Del Valle DM, et al. (2020) An inflammatory cytokine signature predicts COVID-19 severity and survival. Nature Medicine, 26: 1636–43.

14. Tay MZ, et al. (2020) The trinity of COVID-19: Immunity, inflammation and intervention. Nature Rev Immunol, 20: 363–74.

15. Matthay MA, et al. (2020) Acute respiratory distress syndrome. Nature Rev Dis Primers, 6: 18.

16. Fajgenbaum DC, June CH (2020) Cytokine storm. New England J. Medicine, 383: 2255–73.

17. Park A, Iwasaki A (2020). Type I and type III interferons – induction, signaling, and evasion by viruses. Nature Rev Immunol, 20: 543–58.

18. Garvin MR, et al. (2020) A mechanistic model and therapeutic interventions for COVID-19 involving a RAS-mediated bradykinin storm. eLife, 9: e59177.

19. Wautier JL, Wautier MP (2022) Vascular permeability in diseases. Int J Mol Sci, 23: 3645.

20. Curran CS, et al. (2020) COVID-19 usurps host regulatory networks. Front Pharmacol, 11: 1278.

21. Attiq A, et al. (2021) The triumvirate of NF-κB, inflammation and cytokine storm in COVID-19. Int Immunopharmacol, 101: 108255.

22. Coelho SVA, et al. (2024) Potential pathways and pathophysiological implications of viral infection-driven activation of kallikrein–kinin system (KKS). Viruses, 16: 245.

23. de Pascual-Teresa S, et al. (2000) Quantitative analysis of flavan-3-ols in Spanish foodstuffs and beverages. J Agric Food Chem, 48: 5331-7.

24. Kusano R, et al. (2010) α-Amylase and lipase inhibitory activity and structural characterization of Acacia bark proanthocyanidins. J Nat Prod, 74: 119–28,

25. Kuliev R Z, et al. (2004) Dimeric proanthocyanidins from Rhodiola semenovii. Chem Nat Comp, 40: 94–5.

26. Harnly JM, et al. (2006) Flavonoid content of US fruits, vegetables, and nuts. J Agric Food Chem, 54: 9966–77.

27. Mominul IMD, et al. (2025) Stabilizing effect of green tea extract and epigallocatechin-3-gallate (EGCG) on mast cell : an in vivo study. Inflammopharmacol, 33: 4685–701.

28. White HM, et al. (2025) Comparison of culinary and ceremonial matcha green teas: relationship between phytochemical composition and antioxidant properties. J Food Meas Charact, 19: 7070–9.

29. Bai ZZ, et al. (2021) Bioactive components, antioxidant and antimicrobial activities of Paeonia rockii fruit during development. Food Chem, 343: 1.

30. Fukalova TF, et al. (2022) Nutritional Composition, bioactive compounds, and volatiles profile characterization of two edible undervalued plants: Portulaca oleracea L. and Porophyllum ruderale (Jacq.) Cass. Plants, 11: 377.

31. Chakraborty C, et al. (2026) Long COVID-associated neurological symptoms and brain fog: Understanding the mechanism of neuroinflammation, BBB disruption, diagnostics, and therapeutics. Mol Biol Reports, 53: 401.

32. Mohammed HA, et al. (2026) Chemical composition and evaluation of the antibacterial and anti-migratory potentials of Anthemis maritima L. growing in North Africa. BMC Comp Med and Ther, 26: 76.